MICROCOPY RESOLUTION TEST CHART

NATIONAL BUREAU OF STANDARDS-1963-A

DIRECT DETERMINATION OF FLEXURAL
STRAINS IN PLATES USING PROJECTED GRATINGS

BY

C. Y. LIANG, Y. Y. HUNG, A. J. DURELLI AND J. D. HOVANESIAN

SPONSORED BY

OFFICE OF NAVAL RESEARCH
DEPARTMENT OF THE NAVY
WASHINGTON, D.C. 20025

ON

CONTRACT No. N00014-76-C-0487
O.U. PROJECT No. 30339-49
REPORT No. 45

SCHOOL OF ENGINEERING
OAKLAND UNIVERSITY
ROCHESTER, MICHIGAN 48063

JUNE 1977

DIRECT DETERMINATION OF FLEXURAL
STRAINS IN PLATES USING PROJECTED GRATINGS

by

C. Y. Liang, Y. Y. Hung, A. J. Durelli and J. D. Hovanesian

Sponsored by

Office of Naval Research
Department of the Navy
Washington, D.C. 20025

on

Contract No. N00014-76-C-0487
O.U. Project No. 30339-49
Report No. 45

School of Engineering
Oakland University
Rochester, Michigan 48063

June 1977

DIRECT DETERMINATION OF FLEXURAL
STRAINS IN PLATES USING PROJECTED GRATINGS

by

C. Y. Liang, Y. Y. Hung, A. J. Durelli, J. D. Hovanesian

Abstract

It is proposed in this paper to use projected gratings to determine
principal strains in plates subjected to bending. The method requires the
rotation of one photograph of the deformed grating over a copy of itself,
the rotation taking place about the point at which the bending strains
are desired. The idea previously suggested by Stetson to double differen-
tiate holograms of bent plates has been extended and verified with an
application to a plate subjected to twisting. The proposed method is easy
to use and permits the determination of principal strains in plates sub-
jected to much larger deflections than the ones that can be studied using
holograms. Suggestions to improve the precision of the determination are
also made.

Previous Technical Reports to the Office of Naval Research

1. A. J. Durelli, "Development of Experimental Stress Analysis Methods to Determine Stresses and Strains in Solid Propellant Grains"--June 1962. Developments in the manufacturing of grain-propellant models are reported. Two methods are given: a) cementing routed layers and b) casting.

2. A. J. Durelli and V. J. Parks, "New Method to Determine Restrained Shrinkage Stresses in Propellant Grain Models"--October 1962. The birefringence exhibited in the curing process of a partially restrained polyurethane rubber is used to determine the stress associated with restrained shrinkage in models of solid propellant grains partially bonded to the case.

3. A. J. Durelli, "Recent Advances in the Application of Photoelasticity in the Missile Industry"--October 1962. Two- and three-dimensional photoelastic analysis of grains loaded by pressure and by temperature are presented. Some applications to the optimization of fillet contours and to the redesign of case joints are also included.

4. A. J. Durelli and V. J. Parks, "Experimental Solution of Some Mixed Boundary Value Problems"--April 1964. Means of applying known displacements and known stresses to the boundaries of models used in experimental stress analysis are given. The application of some of these methods to the analysis of stresses in the field of solid propellant grains is illustrated. The presence of the "pinching effect" is discussed.

5. A. J. Durelli, "Brief Review of the State of the Art and Expected Advance in Experimental Stress and Strain Analysis of Solid Propellant Grains"-- April 1964. A brief review is made of the state of the experimental stress and strain analysis of solid propellant grains. A discussion of the prospects for the next fifteen years is added.

6. A. J. Durelli, "Experimental Strain and Stress Analysis of Solid Propellant Rocket Motors"--March 1965. A review is made of the experimental methods used to strain-analyze solid propellant rocket motor shells and grains when subjected to different loading conditions. Methods directed at the determination of strains in actual rockets are included.

7. L. Ferrer, V. J. Parks and A. J. Durelli, "An Experimental Method to Analyze Gravitational Stresses in Two-Dimensional Problems"--October 1965. Photoelasticity and moiré methods are used to solve two-dimensional problems in which gravity-stresses are present.

8. A. J. Durelli, V. J. Parks and C. J. del Rio, "Stresses in a Square Slab
    Bonded on One Face to a Rigid Plate and Shrunk"--November 1965.
    A square epoxy slab was bonded to a rigid plate on one of its faces in
    the process of curing. In the same process the photoelastic effects
    associated with a state of restrained shrinkage were "frozen-in."
    Three-dimensional photoelasticity was used in the analysis.

9. A. J. Durelli, V. J. Parks and C. J. del Rio, "Experimental Determination
    of Stresses and Displacements in Thick-Wall Cylinders of Complicated
    Shape"--April 1966.
    Photoelasticity and moiré are used to analyze a three-dimensional rocket
    shape with a star shaped core subjected to internal pressure.

10. V. J. Parks, A. J. Durelli and L. Ferrer, "Gravitational Stresses
    Determined Using Immersion Techniques"--July 1966.
    The methods presented in Technical Report No. 7 above are extended to
    three-dimensions. Immersion is used to increase response.

11. A. J. Durelli and V. J. Parks. "Experimental Stress Analysis of Loaded
    Boundaries in Two-Dimensional Second Boundary Value Problems"--
    February 1967.
    The pinching effect that occurs in two-dimensional bonding problems,
    noted in Reports 2 and 4 above, is analyzed in some detail.

12. A. J. Durelli, V. J. Parks, H. C. Feng and F. Chiang, "Strains and
    Stresses in Matrices with Inserts,"-- May 1967.
    Stresses and strains along the interfaces, and near the fiber ends, for
    different fiber end configurations, are studied in detail.

13. A. J. Durelli, V. J. Parks and S. Uribe, "Optimization of a Slot End
    Configuration in a Finite Plate Subjected to Uniformly Distributed
    Load,"--June 1967.
    Two-dimensional photoelasticity was used to study various elliptical ends
    to a slot, and determine which would give the lowest stress concentration
    for a load normal to the slot length.

14. A. J. Durelli, V. J. Parks and Han-Chow Lee, "Stresses in a Split
    Cylinder Bonded to a Case and Subjected to Restrained Shrinkage,"--
    January 1968.
    A three-dimensional photoelastic study that describes a method and
    shows results for the stresses on the free boundaries and at the
    bonded interface of a solid propellant rocket.

15. A. J. Durelli, "Experimental Stress Analysis Activities in Selected
    European Laboratories"--August 1968.
    This report has been written following a trip conducted by the author
    through several European countries. A list is given of many of the
    laboratories doing important experimental stress analysis work and of
    the people interested in this kind of work. An attempt has been made
    to abstract the main characteristics of the methods used in some of
    the countries visited.

16. V. J. Parks, A. J. Durelli and L. Ferrer, "Constant Acceleration Stresses in a Composite Body"--October 1968.
    Use of the immersion analogy to determine gravitational stresses in two-dimensional bodies made of materials with different properties.

17. A. J. Durelli, J. A. Clark and A. Kochev, "Experimental Analysis of High Frequency Stress Waves in a Ring"--October 1968.
    A method for the complete experimental determination of dynamic stress distributions in a ring is demonstrated. Photoelastic data is supplemented by measurements with a capacitance gage used as a dynamic lateral extensometer.

18. J. A. Clark and A. J. Durelli, "A Modified Method of Holographic Interferometry for Static and Dynamic Photoelasticity"--April 1968.
    A simplified absolute retardation approach to photoelastic analysis is described. Dynamic isopachics are presented.

19. J. A. Clark and A. J. Durelli, "Photoelastic Analysis of Flexural Waves in a Bar"--May 1969.
    A complete direct, full-field optical determination of dynamic stress distribution is illustrated. The method is applied to the study of flexural waves propagating in a urethane rubber bar. Results are compared with approximate theories of flexural waves.

20. J. A. Clark and A. J. Durelli, "Optical Analysis of Vibrations in Continuous Media"--June 1969.
    Optical methods of vibration analysis are described which are independent of assumptions associated with theories of wave propagation. Methods are illustrated with studies of transverse waves in prestressed bars, snap loading of bars and motion of a fluid surrounding a vibrating bar.

21. V. J. Parks, A. J. Durelli, K. Chandrashekhara and T. L. Chen, "Stress Distribution Around a Circular Bar, with Flat and Spherical Ends, Embedded in a Matrix in a Triaxial Stress Field"--July 1969.
    A Three-dimensional photoelastic method to determine stresses in composite materials is applied to this basic shape. The analyses of models with different loads are combined to obtain stresses for the triaxial cases.

22. A. J. Durelli, V. J. Parks and L. Ferrer, "Stresses in Solid and Hollow Spheres Subjected to Gravity or to Normal Surface Tractions"--October 1969.
    The method described in Report No. 10 above is applied to two specific problems. An approach is suggested to extend the solutions to a class of surface traction problems.

23. J. A. Clark and A. J. Durelli, "Separation of Additive and Subtractive Moiré Patterns"--December 1969.
    A spatial filtering technique for adding and subtracting images of several gratings is described and employed to determine the whole field of Cartesian shears and rigid rotations.

24.   R. J. Sanford and A. J. Durelli, "Interpretation of Fringes in Stress-
      Holo-Interferometry"--July 1970.
      Errors associated with interpreting stress-holo-interferometry patterns
      as the superposition of isopachics (with half order fringe shifts) and
      isochromatics are analyzed theoretically and illustrated with computer
      generated holographic interference patterns.

25.   J. A. Clark, A. J. Durelli and P. A. Laura, "On the Effect of Initial
      Stress on the Propagation of Flexural Waves in Elastic Rectangular
      Bars"--December 1970.
      Experimental analysis of the propagation of flexural waves in prismatic,
      elastic bars with and without prestressing. The effects of prestressing
      by axial tension, axial compression and pure bending are illustrated.

26.   A. J. Durelli and J. A. Clark, "Experimental Analysis of Stresses in a
      Buoy-Cable System Using a Birefringent Fluid"--February 1971.
      An extension of the method of photoviscous analysis is presented which
      permits quantitative studies of strains associated with steady state
      vibrations of immersed structures. The method is applied in an
      investigation of one form of behavior of buoy-cable systems loaded by
      the action of surface waves.

27.   A. J. Durelli and T. L. Chen, "Displacements and Finite-Strain Fields in
      a Sphere Subjected to Large Deformations"--February 1972.
      Displacements and strains (ranging from 0.001 to 0.50) are determined in
      a polyurethane sphere subjected to several levels of diametral compression.
      A 500 lines-per-inch grating was embedded in a meridian plane of the
      sphere and moiré effect produced with a non-deformed master. The maximum
      applied vertical displacement reduced the diameter of the sphere by 27
      per cent.

28.   A. J. Durelli and S. Machida, "Stresses and Strain in a Disk with Variable
      Modulus of Elasticity"--March 1972.
      A transparent material with variable modulus of elasticity has been
      manufactured that exhibits good photoelastic properties and can also be
      strain analyzed by moiré. The results obtained suggests that the stress
      distribution in the homogeneous disk. It also indicates that the strain
      fields in both cases are very different, but that it is possible, approxi-
      mately, to obtain the stress field from the strain field using the value
      of E at every point, and Hooke's law.

29.   A. J. Durelli and J. Buitrago, "State of Stress and Strain in A Rectangular
      Belt Pulled Over a Cylindrical Pulley"--June 1972.
      Two- and three-dimensional photoelasticity as well as electrical strain
      gages, dial gages and micrometers are used to determine the stress
      distribution in a belt-pulley system. Contact and tangential stress for
      various contact angles and friction coefficients are given.

30. T. L. Chen and A. J. Durelli, "Stress Field in a Sphere Subjected to Large Deformations"--June 1972.
    Strain fields obtained in a sphere subjected to large diametral compressions from a previous paper were converted into stress fields using two approaches. First, the concept of strain-energy function for an isotropic elastic body was used. Then the stress field was determined with the Hookean type natural stress-natural strain relation. The results so obtained were also compared.

31. A. J. Durelli, V. J. Parks and H. M. Hasseem, "Helices Under Load"--July 1973.
    Previous solutions for the case of close coiled helical springs and for helices made of thin bars are extended. The complete solution is presented in graphs for the use of designers. The theoretical development is correlated with experiments.

32. T. L. Chen and A. J. Durelli, "Displacements and Finite Strain Fields in a Hollow Sphere Subjected to Large Elastic Deformations"--September 1973.
    The same methods described in No. 27, were applied to a hollow sphere with an inner diameter one half the outer diameter. The hollow sphere was loaded up to a strain of 30 per cent on the meridian plane and a reduction of the diameter by 20 per cent.

33. A. J. Durelli, H. H. Hasseem and V. J. Parks, "New Experimental Method in Three-Dimensional Elastostatics"--December 1973.
    A new material is reported which is unique among three-dimensional stress-freezing materials, in that, in its heated (or rubbery) state it has a Poisson's ratio which is appreciably lower than 0.5. For a loaded model, made of this material, the unique property allows the direct determination of stresses from strain measurements taken at interior points in the model.

34. J. Wolak and V. J. Parks, "Evaluation of Large Strains in Industrial Applications"--April 1974.
    It was shown that Mohr's circle permits the transformation of strain from one axis of reference to another, irrespective of the magnitude of the strain, and leads to the evaluation of the principal strain components from the measurement of direct strain in three directions.

35. A. J. Durelli, "Experimental Stress Analysis Activities in Selected European Laboratories"--April 1975.
    Continuation of Report No. 15 after a visit to Belgium, Holland, Germany, France, Turkey, England and Scotland.

36. A. J. Durelli, V. J. Parks and J. O. Bühler-Vidal, "Linear and Non-linear Elastic and Plastic Strains in a Plate with a Big Hole Loaded Axially in its Plane"--July 1975.
    Strain analysis of the ligament of a plate with a big hole indicates that both geometric and material non-linearity may take place. The strain concentration factor was found to vary from 1 to 2 depending on the level of deformation.

37. A. J. Durelli, V. Pavlin, J. O. Bühler-Vidal and G. Ome, "Elastostatics of a Cubic Box Subjected to Concentrated Loads"--August 1975. Analysis of experimental strain, stress and deflection of a cubic box subjected to concentrated loads applied at the center of two opposite faces. The ratio between the inside span and the wall thickness was varied between approximately 5 and 121.

38. A. J. Durelli, V. J. Parks and J. O. Bühler-Vidal, "Elastostatics of Cubic Boxes Subjected to Pressure"--March 1976. Experimental analysis of strain, stress and deflections in a cubic box subjected to either internal or external pressure. Inside span-to-wall thickness ratio varied from 5 to 14.

39. Y. Y. Hung, J. D. Hovanesian and A. J. Durelli, "New Optical Method to Determine Vibration-Induced Strains with Variable Sensitivity After Recording"--November 1976. A steady state vibrating object is illuminated with coherent light and its image slightly misfocused. The resulting specklegram is "time-integrated" as when Fourier filtered gives derivatives of the vibrational amplitude.

40. Y. Y. Hung, C. Y. Liang, J. D. Hovanesian and A. J. Durelli, "Cyclic Stress Studies by Time-Averaged Photoelasticity"--November 1976. "Time-averaged isochromatics" are formed when the photographic film is exposed for more than one period. Fringes represent amplitudes of the oscillating stress according to the zeroth order Bessel function.

41. Y. Y. Hung, C. Y. Liang, J. D. Hovanesian and A. J. Durelli, "Time-Averaged Shadow Moiré Method for Studying Vibrations"--November 1976. Time-averaged shadow moiré permits the determination of the amplitude distribution of the deflection of a steady vibrating plate.

42. J. Buitrago and A. J. Durelli, "On the Interpretation of Shadow-Moiré Fringes"--April 1977. Possible rotations and translations of the grating are considered in a general expression to interpret shadow-moiré fringes and on the sensitivity of the method. Application to an inverted perforated tube.

43. J. der Hovanesian, "18th Polish Solid Mechanics Conference." Published in European Scientific Notes of the Office of Naval Research, in London, England, Dec. 31, 1976. Comments on the planning and organization of, and scientific content of paper presented at the 18th Polish Solid Mechanics Conference held in Wisla-Jawornik from September 7-14, 1976.

44. A. J. Durelli, "The Difficult Choice," -- May 1977. The advantages and limitations of methods available for the analyses of displacements, strain, and stresses are considered. Comments are made on several theoretical approaches, in particular approximate methods, and attention is concentrated on experimental methods: photo-elasticity, moiré, brittle and photoelastic coatings, gages, grids, holography and speckle to solve two- and three-dimensional problems in elasticity, plasticity, dynamics and anisotropy.

Nomenclature

a_n minimum diameter of ellipse or hyperbola associated with fringe order n

b_n maximum diameter of ellipse or hyperbola associated with fringe order n

E modulus of elasticity

h distance of plate surface from neutral axis

$I(x,y)$ light intensity distribution of undeformed plate

$I'(x,y)$ light intensity distribution of deformed plate

n fringe order

p pitch of grating

t thickness of test plate

$T(x,y)$ intensity transmittance of photographic plate recording

$T'(x,y)$ intensity transmittance of contact copy

$w(x,y)$ deformation function corrected

x,y,z co-ordinates

$\varepsilon_1, \varepsilon_2$ maximum and minimum principal strain, respectively.

θ angle between normal to the test plate and viewing direction of camera.

ν Poisson's ratio

σ_1, σ_2 maximum and minimum principal stress, respectively

ϕ angle denoting the orientation of principal direction.

DIRECT DETERMINATION OF FLEXURAL
STRAINS IN PLATES USING PROJECTED GRATINGS

Introduction

Plates are frequently used in engineering to resist bending loads.
Depending on geometry and loading conditions, plates may be difficult to
analyze mathematically. Experimental techniques are then useful. Mechanical
and electrical strain gages give strains at the two faces of the plate, and
from these strains moments can be computed directly. However, this infor-
mation is obtained only point-by-point. Optical methods are more interesting
because they give whole field information, and because no contact with the
plates is required[1]. Of particular importance for this application are
the projected grating,[2,3] Ligtenberg's[4] and Salet-Ikeda techniques,[5]
holographic[6,7] and speckle-shearing interferometry[8]. All these optical
methods measure either deflections or slope of deflections; thus it is
necessary to differentiate the information once, or twice, to obtain the
bending strains. These operations besides being very laborious are a source
of error. The results obtained using these methods are also subjected to
the limitations of the theory of plates. One of the authors used gratings
directly printed on the surface of the plate and a superposed master grating
to produce moiré.[9] Whole-field in-plane displacements are obtained this
way and only one differentiation is required to obtain strains, but the
method has not been applied yet to vibrations and is limited to relatively
small deflections.

An innovative idea was introduced by Stetson[10] whereby bending moments
can be determined directly using holographic interferometry. The method
consists in superposing and aligning two identical transparencies of the
fringe pattern of deflections obtained by holographic interferometry.

-1-

By rotating one transparency through an angle of 180° (in the plane of the film) with respect to the other about a point of interest, a moiré in the form of either an ellipse or a hyperbola is produced. Stetson showed that the directions and the length of the principal axes of these figures indicate the directions and the magnitude of the principal strians, respectively. Also, the relative sign of the two principal strains can be obtained from the form of the moiré pattern. An ellipse indicates that the principal strains are of the same sign. Opposite signs correspond to the hyberbola. The method permits only point-by-point analysis, but it is the only one so far developed for double differentiation.

The present paper extends the Stetson's idea to the projected grating method. While the hologram interferometry is mainly suitable for measuring very small deflections, the projected grating method can be used to determine relatively large ones. The paper includes considerations on the error inherent in the double differentiation operation and suggests how the results can be improved. A verification is also given.

Description of the Method

A grating is projected onto the plate (Fig. 1), in a direction making an angle θ with the normal to the plate. The projection may be achieved by using either a projector[2] or by interference of two coherent beams[3]. When the plate is deformed, the shadow of the grating on the surface of the plate is perturbated because of the deflection. The perturbated grating is photographed by a camera viewing normally and is recorded on a photographic plate. A contact copy of the recorded grating is made on a second plate. The two plates are superposed and carefully aligned so that no moiré is seen. One of the plates is then rotated 180° about a point of interest. A moiré will appear in the shape of an ellipse or a hyberbola.

Analysis

The light intensity distribution of a sinusoidal grating projected onto a
flat plate can be represented by:

$$I(x,y) = 1 + \cos \frac{2\pi}{p} x \tag{1}$$

where $I(x,y)$ is the intensity distribution; p is the grating pitch observed
on the plate. The grating is running parallel to the y-axis. When the plate
is deformed, the grating will be distorted accordingly and its intensity
distribution becomes:

$$I'(x,y) = 1 + \cos \frac{2\pi}{p} [x - w(x,y) \cdot \tan\theta] \tag{2}$$

where $I'(x,y)$ is the distorted grating intensity; θ is the angle between the
direction of projection and the normal to the plate, and $w(x,y)$ is the
deflection of the plate.

Assuming negative and linear recording, the intensity transmittance
$T(x,y)$ of the photographic plate recording the intensint of Eq. (2) is:

$$T(x,y) = 1 - \cos \frac{2\pi}{p} [x - w(x,y) \cdot \tan\theta] \tag{3}$$

and the intensity transmittance $T'(s,y)$ of the contact copy is:

$$T'(x,y) = 1 + \cos \frac{2\pi}{p} [x - w(x,y) \cdot \tan\theta] \tag{4}$$

The intensity transmittance of the two transparencies superposed and aligned is
represented by the product of the individual transmittances. With one plate
being rotated 180°, and choosing the point of rotation as the origin, the
resulting intensity transmittance $T_R(x,y)$ is given by:

$$T_R(x,y) = T(x,y) \cdot T'(-x,-y) \tag{5}$$

The above equation can be expanded to yield:

$$T_R(x,y) = 1 + \frac{1}{2} \cos\left\{\frac{2\pi}{p} \tan\theta [w(x,y) + w(-x,-y)]\right\}$$

$$- \cos \frac{2\pi}{p} [x - w(x,y)\tan\theta] + \cos \frac{2\pi}{p} [-x - w(-x,-y)\tan\theta]$$

$$- \frac{1}{2} \cos \frac{2\pi}{p} [2x - w(x,y)\tan\theta + w(-x,-y)\tan\theta] \tag{6}$$

Except for the first two terms, all the terms in the above equation are of high spatial frequency.

If the pair of plates is illuminated by a uniform intensity quasi plane wave of unity magnitude, and if one considers the average illuminence over a resolution cell ΔA, the resulting transmitted intensity field I_o may be represented by:

$$I_o(x,y) = 1 + \frac{1}{2} \cos \left[\frac{2\pi}{p} \tan\theta [w(x,y) + w(-x,-y)]\right] \tag{7}$$

In Eq. (7), the linear dimensions of ΔA are considered to be large compared to the grating pitch p. Dark fringes form when

$$\frac{2\pi}{p} \tan\theta [w(x,y) + w(-x,-y)] = n\pi \tag{8}$$

where $n = 1, 3, 5, 7, 9, \ldots \ldots$, is the fringe order.

By Taylor's series expansion about the origin and terminating at the fourth term, $w(x,y)$ can be expressed as

$$w(x,y) = w(0,0) + \left[x \frac{\partial w(0,0)}{\partial x} + y \frac{w(0,0)}{\partial y}\right]$$

$$+ \frac{1}{2!} \left[x^2 \frac{\partial^2 w(0,0)}{\partial x^2} + 2xy \frac{\partial^2 w(0,0)}{\partial x \partial y} + y^2 \frac{\partial^2 w(0,0)}{\partial^2 y}\right.$$

$$+ \frac{1}{3!} \left[x^3 \frac{\partial^3 w(0,0)}{\partial x^3} + 3x^2 y \frac{\partial^3 w(0,0)}{\partial x^2 \partial y} + 3xy^2 \frac{\partial^3 w(0,0)}{\partial x \partial y^2}\right.$$

$$\left. + y^3 \frac{\partial^3 w(0,0)}{\partial y^3}\right] \tag{9}$$

and

$$w(-x,-y) = w(0,0) + [-x \frac{\partial w(0,0)}{\partial x} - y \frac{\partial w(0,0)}{\partial y}]$$

$$+ \frac{1}{2!} [x^2 \frac{\partial^2 w(0,0)}{\partial x^2} + 2xy \frac{\partial^2 w(0,0)}{\partial x \partial y} + y^2 \frac{\partial^2 w(0,0)}{\partial y^2}]$$

$$+ \frac{1}{3!} [-x^3 \frac{\partial^3 w(0,0)}{\partial x^3} - 3x^2 y \frac{\partial^3 w(0,0)}{\partial x^2 \partial y} - 3xy^2 \frac{\partial^3 w(0,0)}{\partial x \partial y^2}$$

$$- y^3 \frac{\partial^3 w(0,0)}{\partial y^3}] \tag{10}$$

Define the origin such that $w(0,0) = 0$. If the orientation of the coordinate axes is chosen such that one of the partial derivatives of $w(0,0)$ vanishes, then the crossed partial derivative $\partial^2 w(0,0)/\partial x \partial y$ would vanish as well. Under these conditions,

$$w(x,y) - w(-x,-y) = x^2 \frac{\partial^2 w(0,0)}{\partial x^2} + y^2 \frac{\partial^2 w(0,0)}{\partial y^2} \tag{11}$$

and Eq. (8) can be written as

$$x^2 \frac{\partial^2 w(0,0)}{\partial x^2} + y^2 \frac{\partial^2 w(0,0)}{\partial y^2} = \frac{np}{2\tan\theta} \tag{12}$$

The above equation represents an ellipse or a hyperbola depending on the relative signs of $\partial^2 w(0,0)/\partial x^2$ and $\partial^2 w(0,0)/\partial y^2$. Since the cross derivative $\partial w(0,0)/\partial x \partial y$ is zero, $\partial^2 w(0,0)/\partial x^2$ and $\partial^2 w(0,0)/\partial y^2$ measure the principal bending strains at the origin, the point about which the photographic plates is rotated. They are related to the principal diameters of the ellipse or hyperbola by:

$$\frac{\partial^2 w(0,0)}{\partial x^2} = \frac{np}{2\tan\theta} \cdot \frac{1}{a_n^2} \tag{13}$$

$$\frac{\partial^2 w(0,0)}{\partial y^2} = \frac{np}{2\tan\theta} \cdot \frac{1}{b_n^2} \tag{14}$$

where $2 a_n$ and $2 b_n$ are the principal diameters associated with finge order n.

By measuring the principal diameters, the principal bending strain can be calculated by the following equations

$$\varepsilon_1 = h \frac{\partial^2 w(0,0)}{\partial x^2} = h\frac{np}{2\tan\theta} \cdot \frac{1}{a_n^2} \tag{15}$$

and

$$\varepsilon_2 = h \frac{\partial^2 w(0,0)}{\partial y^2} = h \frac{np}{2\tan\theta} \cdot \frac{1}{b_n^2} \tag{16}$$

where h is the distance from the neutral axis to the plate surface, and ε_1 and ε_2 are the maximum and minimum principal strains, respectively. The directions of the principal strains are indicated by the orientation of the principal diameters. To use Eqs. (15) and (16), it is necessary to obtain values of $\frac{n}{a_n^2}$ and $\frac{n}{b_n^2}$ as near to the point of interest as possible. Precisely at the origin, both n and a_n (or b_n) approach zero, therefore the ratios become mathematically indeterminate.

To increase the precision of the procedure it is advisable to determine the limit of the above ratios. As one moves along a major diameter, away from the origin, values of $\frac{1}{a_1}$, $\frac{3}{a_2}$ . . . . $\frac{n}{a_n}$ can be computed. A graphical extrapolation of these ratios to the origin is herein proposed as a means to estimate $\frac{n}{a_n^2}$ as n approaches zero. This procedure was used in the next section for the experimental verification.

The above analysis is based on a sinusoidal grating. Should a square wave grating be used, the same result with better fringe visibility will be obtained. [10]

Experimental Verification

A thin flat titanium alloy plate clamped along one side was chosen for demonstration. The plate measures 12.7 cm x 12.7 cm x 0.394 mm. Two point loads, acting in parallel but opposite direction, were applied to the test plate at locations (1) and (2) shown in Fig. 2. A grating of 16.5 lines/cm was projected onto the plate with $\theta = 45°$. Kodak contrast process films were used for recording and copying. Figure 2 shows the test plate under loading with the grating projected on it.

In order to compare the results obtained by the proposed moiré method with the well-established electrical resistance strain gage techniques, three rectangular strain rosettes were mounted at three selected points on the plate. The exact locations of these points are shown on Fig. 2.

The pitch of the grating was first determined from a photograph of the projected grating on the undeformed test plate. The loading was then applied, and the grating on the deformed plate was photographed. Strain measurements were made before and after the photographic recording.

The experimental data obtained by the moiré method were processed in the manner as described earlier in the text. Equations (15) and (16) were employed to calculate the maximum principal strains, and h was taken to be half the thickness of the test plate.

Results and Discussion

A summary of the experimental results is presented in Table 1. Figure 3(a) shows the elliptical moiré fringe pattern at point A on the test plate while Fig. 3(b) reveals the case of hyperbolic bending at point B. As can be observed in Table 1, the maximum principal strain and orientation of the principal direction obtained by the moiré method check well with those obtained by strain gage measurements, but the discrepancy in the case of the minimum principal strain measurements is larger. The value of the minimum strain is small and larger difference with strain gage results could be expected. The sources of error will be discussed below.

One of the major sources of error comes from the fact that the governing Eqs. (13) and (14) are based on a four term Taylor expansion of the deformation function $w(x,y)$ and $w(-x,-y)$ in Eqs. (9) and (10). The curvature at the center of the ellipse (or hyperbola) is determined from measurements at the extremities of the ellipse (or hyperbola). Therefore, it can be expected that the errors will grow with increase in the principal diameters. This kind of error can be reduced by increasing the density of the projected grating. Another way to improve the accuracy of the measurement is to estimate the principal strains at the center of rotation by means of the extrapolation explained earlier. Figure 4 presents a graph of principal strains for point B determined from fringe orders taken at different diameters. By means of extrapolation it is estimated that $|\varepsilon_1| = 617 \times 10^{-6}$ and $|\varepsilon_2| = 230 \times 10^{-6}$. These results check quite well with those obtained from strain gages (see table 1).

It is assumed in the analysis of the proposed moiré method that the plate is initially flat. In fact, Eqs. (13) and (14) predict the principal

-8-

curvatures of the plate at the point of interest due to bending only. Any initial curvatures in the test plate would cause errors in the final determination.

When this proposed moiré method is used, care should be exercised in the initial alignment and subsequent rotation of the photographs. In the present experiment, this important step of data reduction was carried out on a piece of ground glass sitting on a uniform light source. The two photographic plates were aligned such that the recorded grating patterns coincided with each other. This condition was ensured by the absence of moiré fringes. When one of the photographic plates was rotated, the angle of rotation would be 180° when the light intensity at and near the point of rotation reached a maximum value. This condition can be ensured, for example, by employing a light meter to continuously monitor the light intensity at the point of rotation.

One major advantage of this method over the conventional strain gage technique is that the strain at any point of the plate can be determined from a single photographic record. The experimental technique is easy to apply, and unlike some other optical methods which require expensive optical equipment, this experiment can be performed with just a projector, a master grating and a camera. Although only the absolute values and the relative signs of the principal strains can be determined using this method, the actual signs of the strains at any point of the plate can be determined if the data reduction is started at a point at which the strain sign is independently known.

While holographic interferomety[10] can be used to study bending strains due to very small deformation, the proposed moiré method using a projected grating is suitable for the determination of bending strains of relatively

-9-

large magnitude. Since the quality of the photographic recording of the projected grating is inherently superior to that of the holographic fringes, the moiré pattern obtained by the projected grating method is of much better visibility, as evidenced by the results presented in Fig. 3.

Conclusion

A technique has been developed to determine bending strains directly using projected gratings. The method is particularly useful to study strains associated with relatively large deflections. The sensitivity of the method is proportional to the density of the projected grating and depends on the resolving capability of the imaging system.

Acknowledgments

References

1. Weller R. and Shepard B. M., "Displacement Measurement by Mechanical Interferometry," _Proceedings Soc. Exp. Stress Analysis_, Vol. 6, P, 1949.

2. Hovanesian J. D. and Hung Y. Y., "Moiré Contour-Sum, Contour Difference and Vibrational Analysis of Arbitrary Objects," _Applied Optics_, Vol. 10 (12), 1971.

3. Vest C. M. and Sweeny D. W., "Measurement of Vibrational Amplitude by Modulation of Projected Fringes," _Applied Optics_, Vol. 11, No. 2, 442, 1972.

4. Ligtenberg F. K., "The Moiré Method: A New Experimental Method for the Determination of Moments in Small Slab Models," _Proc. SESA_ XII (2), 83-89, 1954.

5. Duncan J. P. and Brown C. J. E., "Slope Contours in flexed elastic plates by Salet-Ikeda technique," Proc. First Inter. Cong. Exp. Mechanics, 149-176, 1963.

6. Hovanesian J. D. and Varner J., "Methods for Determining the Bending Moments in Normally Loaded Thin Plates by Hologram Interferometry," Strathclyde Symposium on the Engineering Use of Holography, Cambridge University Press, 1968.

7. Boone P. M. and Verbiest R., "Application of Hologram Interferometry to Plate Deformation and Translation Measurement," Optica Acta, 16, 555-567, Ict. 1969.

8. Hung Y. Y. and Taylor C. E., "Measurement of Slopes of Structural Deflections by Speckle-Shearing Interferometry," _Experimental Mechanics_, Vol. 14, No. 7, 281-285, July 1974.

9. Durelli A. J. and Parks V. J., "Moiré Analysis of Strain," Prentice-Hall

10. Stetson K. A., "Moiré Method for Determining Bnnding Moments from
   Hologram Interferometry," Optics Technology, Vol. 2, pp. 80-84, 1970.

Table 1   Summary of Experimental Results

t = 0.394 mm				$\tan\theta = 1.02$		
h = 0.197 mm				$E = 1.01 \times 10^{11} N/m^2$		
p = 0.605 mm				$\nu = 0.3$		

LOCATION	MEASUREMENT	OPTICAL*				STRAIN GAGE
		$N = 0$**	$N = 1$	$N = 2$	$N = 3$	
A***	a_n, cm	–	0.737	1.25	1.66	–
	b_n, cm	–	2.03	3.58	4.70	–
	$\varepsilon_1 \times 10^6$	1,090	1,100	1,120	1,080	1,020
	$\varepsilon_2 \times 10^6$	150	144	139	135	100
	ϕ, deg	25.3	25.3	25.3	25.3	23.6
	$\sigma_1 \times 10^{-6}, N/m^2$	126	127	131	124	117
	$\sigma_2 \times 10^{-6}, N/m^2$	52.9	52.6	53.4	50.9	45.1
B***	a_n, cm	–	0.996	1.75	2.39	–
	b_n, cm	–	1.53	2.50	3.18	–
	$\varepsilon_1 \times 10^6$	617	600	582	529	636
	$\varepsilon_2 \times 10^6$	230	255	286	295	−216
	ϕ, deg.	45	45	45	45	42.6
	$\sigma_1 \times 10^{-6}, N/m^2$	60.8	58.1	55.1	48.9	63.4
	$\sigma_2 \times 10^{-6}, N/m^2$	5.98	8.30	12.4	15.1	−2.80

* The proposed optical method only determines the absolute values of principal strain

** Values of principal strains at n = 0 are estimated by extrapolation

*** The principal strains and stresses at location A are of the same sign, and those at location B are of the opposite sign.
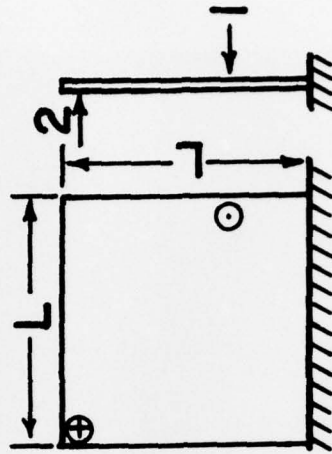
PROJECTED
GRATING

CAMERA
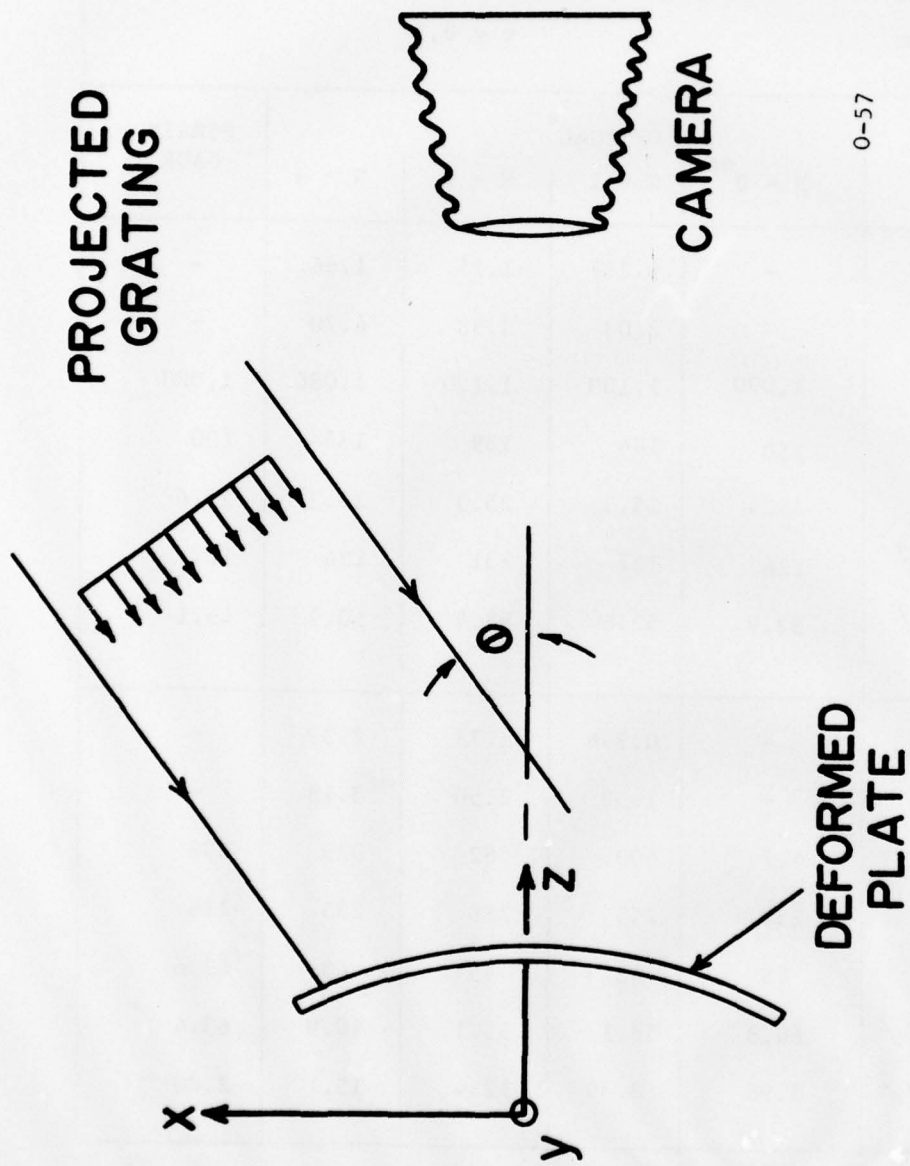
DEFORMED
PLATE

Figure 1 Experimental Set-Up of the Projected Grating Method

+ LOCATION OF STRAIN GAUGES

⊙, ⊕ LOCATION OF POINT LOAD
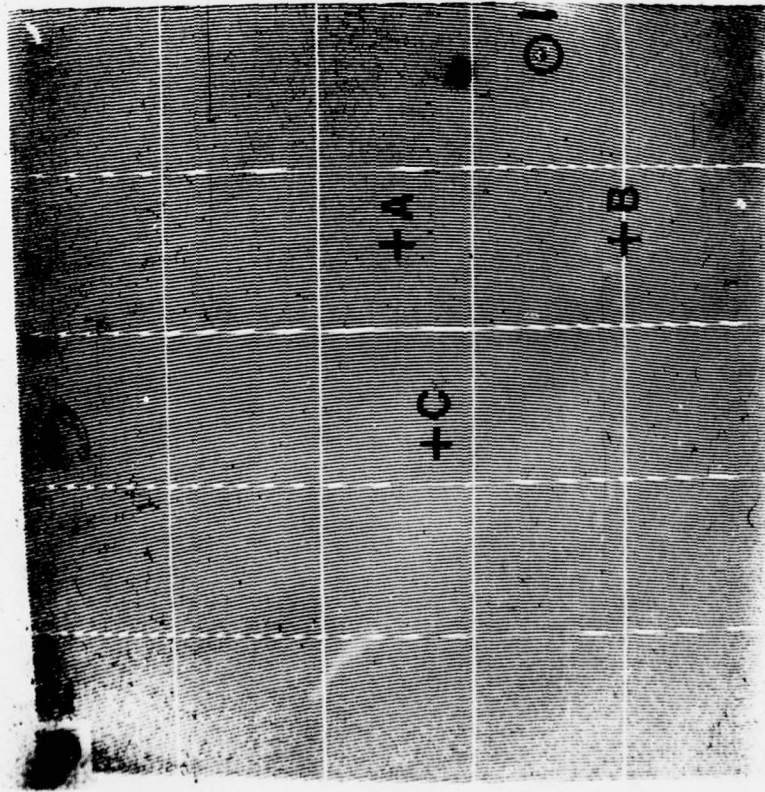
$p = 0.605$ cm
$L = 12.7$ cm

0-58

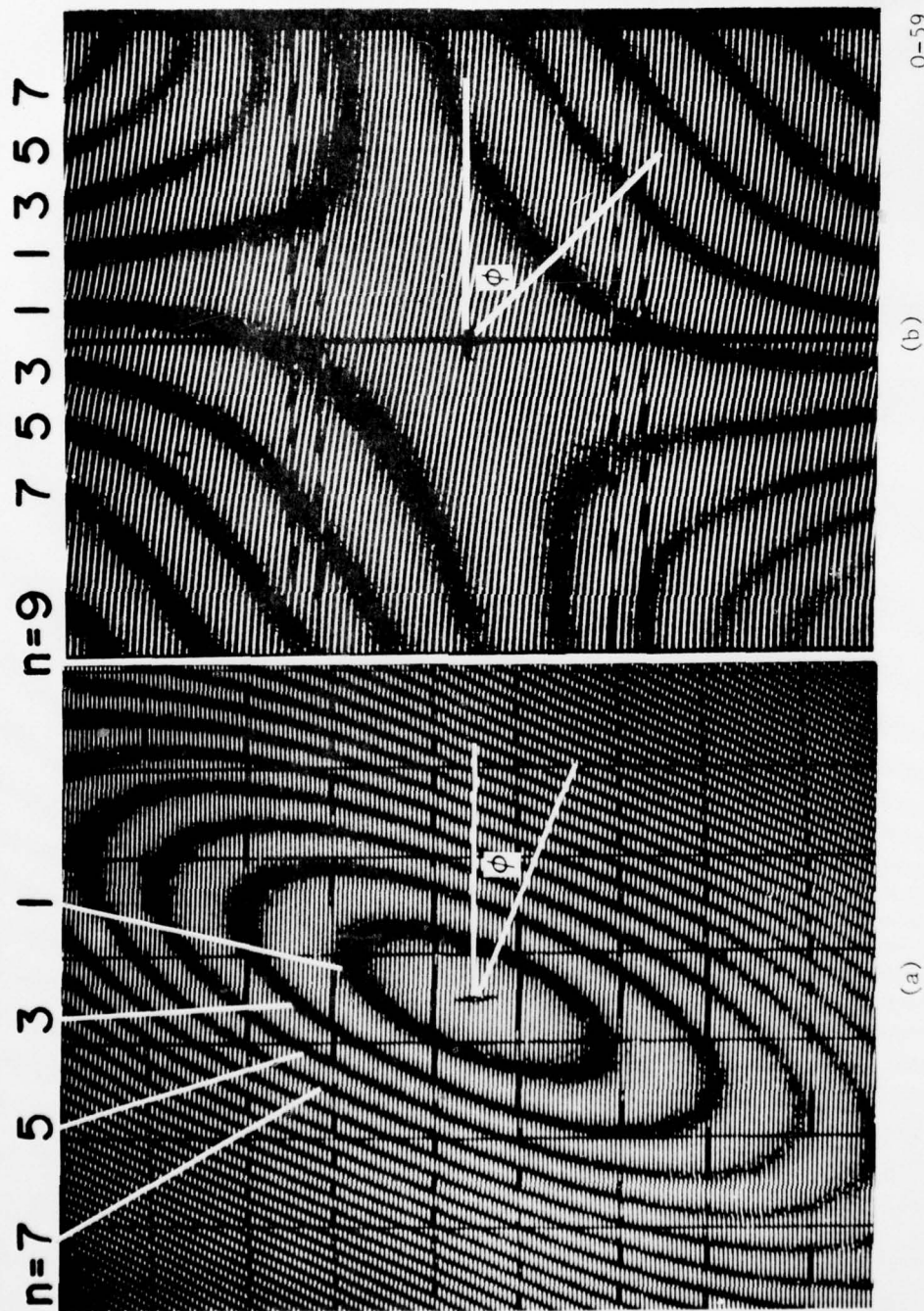Figure 2 Grating Projected on Deformed Plate

Figure 3 Moire Fring Patterns for Double Differentiation of Out-of-Plane Deflection at (a) Point A and (b) Point B on a Plate Subjected to Twisting
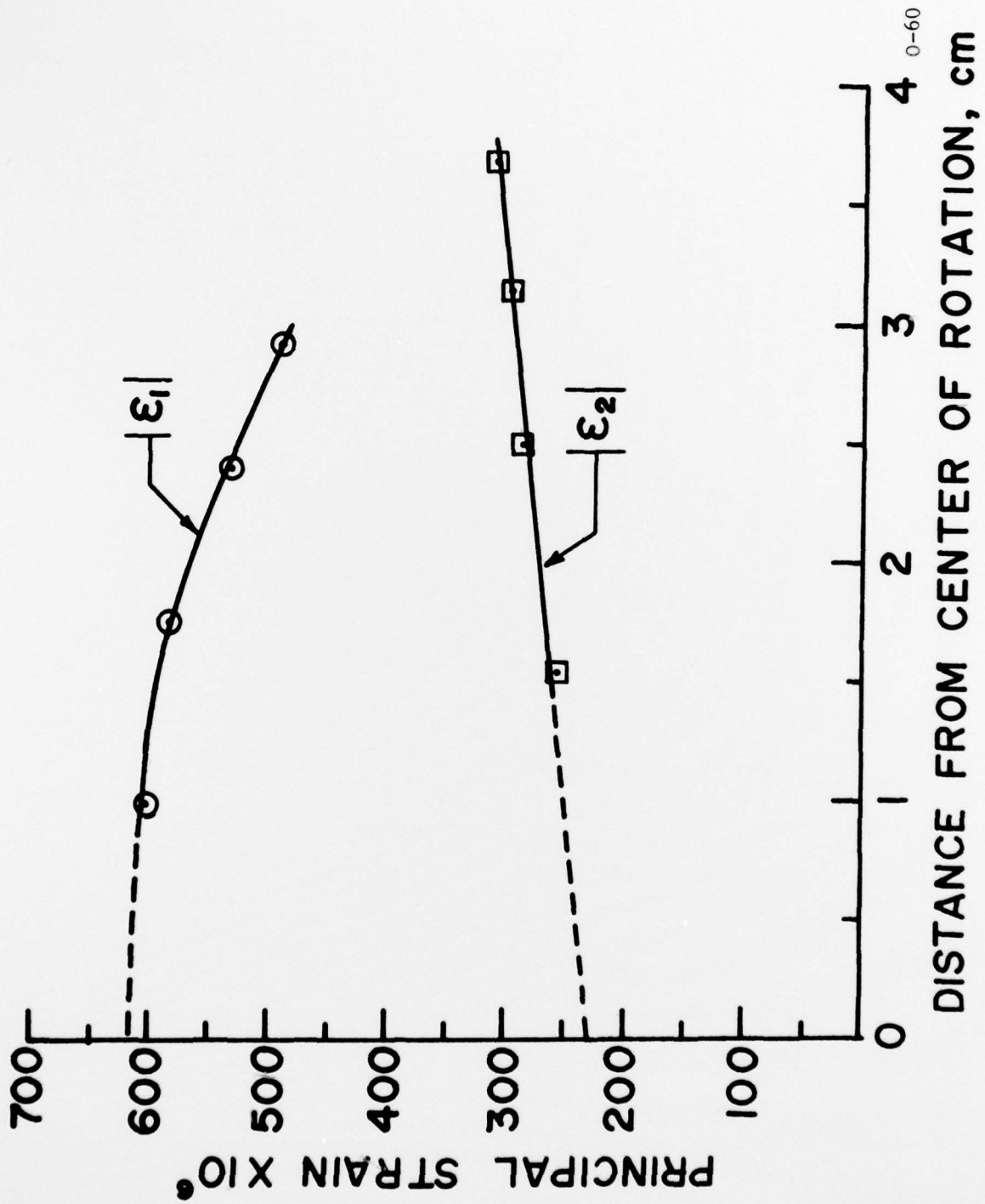
Figure 4 Principal Strain Measured at n = 1, 3, 5, 7 Versus Distance from Center of Rotation at Point B on Test Plate

Part I - Government

Chief of Naval Research
Department of the Navy
Arlingon, Virginia 22217
Attn: Code 474 (2)
              471
              222

Director
ONR Branch Office
495 Summer Street
Boston, Massachusetts 02210

Director
ONR Branch Office
536 S. Clark Street
Chicago, Illinois 60604

Director
Naval Research Laboratory
Attn: Code 2529 (ONRL)
Washington, D.C. 20390 (6)

U.S. Naval Research Laboratory
Attn: Code 2627
Washington, D.C. 20390

Commanding Officer
ONR Branch Office
207 West 24th Street
New York, N.Y. 10011

Director
ONR Branch Office
1030 E. Green Street
Pasadena, California 91101

Defense Documentation Center
Cameron Station
Alexandria, Virginia 22314 (12)

Army

Commanding Officer
U.S. Army Research Off. Durham
Attn: Mr. J. J. Murray
CRD-AA-IP
Box CM, Duke Station
Durham, North Carolina 27706

Commanding Officer
AMXMR-ATL
Attn: Mr. R. Shea
U.S. Army Materials Res. Agency
Watertown, Massachusetts 02172

Watervliet Arsenal
MAGGS Research Center
Watervliet, New York 12189
Attn: Director of Research

Redstone Scientific Info. Center
Chief, Document Section
U.S. Army Missile Command
Redstone Arsenal, Alabama 35809

Army R &D Center
Fort Belvoir, Virginia 22060

Navy

Commanding Officer & Director
Naval Ship Res. & Dev. Center
Bethesda, Maryland 20034
Attn: Code 042 (Tech. Lib. Br.)
              17 (Struc. Mech. Lab.)
              172
              172
              174
              177
              1800(Appl. Math. Lab.)
              5412S (Dr. W.D. Sette)
              19 (Dr. M.M. Sevik)
              1901 (Dr. M. Strassberg)
              1945
              196 (Dr. D. Feit)
              1962

Naval Weapons Laboratory
Dahlgren, Virginia 22448

Naval Research Laboratory
Washington, D.C. 203
Attn: Code 8400
              8410
              8430
              8440
              6300
              6390
              6380

Undersea Explosion Res. Div.
Naval Ship R&D Center
Norfolk Naval Shipyard
Portsmouth, Virginia 23709
Attn: Dr. E. Palmer
       Code 780

Naval Ship Res. & Dev. Center
Annapolis Division
Annapolis, Maryland 21402
Attn: Code 2740 - Dr. Y. F. Wang
             28 - Mr. R.J. Wolfe
             281 - Mr. Niederberger
             2814 - Dr. H. Vanderveldt

Technical Library
Naval Underwater Weapons Center
Pasadena Annex
3202 E. Foothill Blvd.
Pasadena, California 91107

U.S. Naval Weapons Center
China Lake, California 93557
Attn: Code 4062 - Mr. W. Werback
             4520 - Mr. Ken Bischel

Commanding Officer
U.S. Naval Civil Engr. Lab.
Code L31
Port Hueneme, California 93041

Technical Director
U.S. Naval Ordnance Lab.
White Oak
Silver Spring, Maryland 20910

Technical Director
Naval Undersea R&D Center
San Diego, California 92132

Supervisor of Shipbuilding
U.S. Navy
Newport News, Virginia 23607

Techanical Director
Mare Island Naval Shipyard
Vallejo, California 94592

U.S. Navy Underwater Sound Ref.
                              Lab.
Office of Naval Research
P.O. Box 3337
Orlando, Florida 32806

Chief of Naval Operations
Dept. of the Navy
Washington, D.C. 20350
Attn: Code Op07T

Strategic Systems Project Off.
Department of the Navy
Washington, D.C. 20390
Attn: NSP- 001 Chief Scientist

Deep Submergence Systems
Naval Ship Systems Command
Code 39522
Department of the Navy
Washington, D.C. 203 60

Ergineering Dept.
U.S. Naval Academy
Annapolis, Maryland 21402

Naval Air Systems Command
Dept. of the Navy
Washington, D.C. 20360
Attn: NAVAIR 5302 Aero & Struc.
              5308 Struc.
              52031F Materials
              604 Tech. Lib.

Director, Aero Mechanics
Naval Air Development Center
 Jonnsville
Warminster, Pennsylvania 18974

Technical Director
U.S. naval Undersea R&D Center
San Diego, California 92132

Engineering Department
U.S. Naval Academy
Annapolis, Maryland 21402

Naval Facilities Engineering Command
Dept. of the Navy
Washington, D.C. 20360
Attn: NAVFAC 03 Res. & Dev.
              04 Res. & Dev.
              14114 Tech. Lib.

Naval Sea Systems Command
Dept. of the Navy
Washington, D.C. 20360
Attn: NAVSHIP 03 Res. & Tech.
              031 Ch.Scientist R&D
              03412 Hydromechanics
              037 Ship Silencing Div.
              035 Weapons Dynamics

Navy cont.

Naval Ship Engineering Center
Prince George's Plaza
Hyattsville, Maryland 20782
Attn: NAVSEC 6100 Ship Sys Engr &
            Des Dep
        6102C Computer-Aided
            Ship Des
        6105G
        6110 Ship Concept Des
        6120 Hull Div.
        6120D Hull Div.
        6128 Surface Ship
            Struct.
        6129 Submarine Struct.

Air Force

Commander WADD
Wright-Patterson Air Force Base
Dayton, Ohio 45433
Attn: Code WWRMDD
        AFFDL (FDDS)
        Structures Division
        AFLC (MCEEA)

Chief, Applied Mechanics Group
U.S. Air Force Inst. of Tech.
Wright-Patterson Air Force Base
Dayton, Ohio 45433

Chief, Civil Engineering Branch
WLRC, Research Division
Air Force Weapons Laboratory
Kirtland AFB, New Mexico 87117

Air Force Office of Scientific
Research
1400 Wilson Blvd.
Arlington, Virginia 22209
Attn: Mechanics Div.

NASA

Structures Research Division
National Aeronautics & Space Admin.
Langley Research Center
Langley Station
Hampton, Virginia 23365

National Aeronautic & Space Admin.
Associate Administrator for Ad-
vanced Research & Technology
Washington, D.C. 02546

Scientific & Tech. Info. Facility
NASA Representative (S-AK/DL)
P.O. Box 5700
Bethesda, Maryland 20014

Other Government Activities

Commandant
Chief, Testing & Development Div.
U.S. Coast Guard
1300 E. Street, N.W.
Washington, D.C. 20226

Technical Director
Marine Corps Dev & Educ. Command
Quantico, Virginia 22134

Director
National Bureau of Standards
Washington, D.C. 20234
Attn: Mr. B.L. Wilson, EN 219

Dr. M. Gaus
National Science Foundation
Engineering Division
Washington, D.C. 20550

Science & Tech. Division
Library of Congress
Washington, D.C. 20540

Director
Defense Nuclear Agency
Washington, D.C. 20305
Attn: SPSS

Commander Field Command
Defense Nuclear Agency
Sandia Base
Albuquerque, New Mexico 87115

Director Defense Research & Engr
Technical Library
Room 3C-128
The Pentagon
Washington, D.C. 20301

Chief, Airframe & Equipment Branch
FS-120
Office of Flight Standards
Federal Aviation Agency
Washington, D.C. 20553

Chief, Research and Development
Maritime Administration
Washington, D.C. 20235

Deputy Chief, Office of Ship Constr.
Maritime Administration
Washington, D.C. 20235
Attn: Mr. U.L. Russo

Atomic Energy Commission
Div. of Reactor Devel. & Tech.
Germantown, Maryland 20767

Ship Hull Research Committee
National Research Council
National Academy of Sciences
2101 Constitution Avenue
Washington, D.C. 20418
Attn: Mr. A.R. Lytle

Part 2 - Contractors and Other
            Technical Collaborators

Universities

Dr. J. Tinsley Oden
University of Texas at Austin
345 Eng. Science Bldg.
Austin, Texas 78712

Prof. Julius Miklowitz
California Institute of Technology
Div. of Engineering & Applied Sci.
Pasadena, California 91109

Dr. Harold Liebowitz, Dean
School of Engr. & Applied Science
George Washington University
725 - 23rd St., N.W.
Washington, D.C. 20006

Prof. Eli Sternberg
California Institute of Technology
Div. of Engr. & Applied Sciences
Pasadena, California 91109

Prof. Paul M. Naghdi
University of California
Div. of Applied Mechanics
Etcheverry Hall
Berkeley, California 94720

Professor P.S. Symonds
Brown University
Division of Engineering
Providence, R.I. 02912

Prof. A.J. Durelli
John F. Dodge Professor
Oakland University
Rochester, Michigan 48063

Prof. R.B. Testa
Columbia University
Dept. of Civil Engineering
S.W. Mudd Bldg.
New York, New York 10027

Prof. H.H. Bleich
Columbia University
Dept. of Civil Engineering
Amsterdam & 120th St.
New York, New York 10027

Prof. F.L. DiMaggio
Columbia University
Dept. of Civil Engineering
616 Mudd Building
New York, New York 10027

Prof. A.M. Freudenthal
George Washington University
School of Engineering & Applied
                            Science
Washington, D.C. 20006

D.C. Evans
University of Utah
Computer Science Division
Salt Lake City, Utah 84112

Prof. Norman Jones
Massachusetts Inst. of Technology
Dept. of Naval Architecture &
        Marine Engrng
Cambridge, Massachusetts 02139

Asst. to Secretary Defense
Atomic Energy-Att. D. Cotter
Washington, D.C. 20301

Dr. V.R. Hodgson
Wayne State University
School of Medicine
Detroit, Michigan 48202

Dean B.A. Boley
Northwestern University
Technological Institute
2145 Sheridan Road
Evanston, Illinois 60201

Prof. P.G. Hodge, Jr.
University of Minnesota
Dept. of Aerospace Engng & Mech.
Minneapolis, Minnesota 55455

Dr. D.C. Drucker
University of Illinois
Dean of Engineering
Urbana, Illinois 61801

Prof. N.M. Newmark
University of Illinois
Dept. of Civil Engineering
Urbana, Illinois 61801

Prof. E. Reissner
University of California, San Diego
Dept. of Applied Mechanics
La Jolla, California 92037

Prof. William A. Nash
University of Massachusetts
Dept. of Mechanics & Aerospace Eng.
Amherst, Massachusetts 01002

Library (Code 0384)
U.S. Naval Postgraduate School
Monterey, California 93940

Prof. Arnold Allentuch
Newark College of Engineering
Dept. of Mechanical Engineering
323 High Street
Newark, New Jersey 07102

Dr. George Herrmann
Stanford University
Dept. of Applied Mechanics
Stanford, California 94305

Prof. J.D. Achenbach
Northwestern University
Dept. of Civil Engineering
Evanston, Illinois 60201

Director, Applied Research Lab.
Pennsylvania State University
P.O. Box 30
State College, Pennsylvania 16801

Prof. Eugen J. Skudrzyk
Pennsylvania State University
Applied Research Laboratory
Dept. of Physics - P.O. Box 30
State College, Pennsylvania 16801

Prof. J. Kempner
Polytechnic Institute of Brooklyn
Dept. of Aero. Engrg & Applied Mech.
333 Jay Street
Brooklyn, N.Y. 11201

Prof. J. Klosner
Polytechnic Institute of Brooklyn
Dept. of Aerospace & Appl. Mech.
333 Jay Street
Brooklyn, N.Y. 11201

Prof. R.A. Schapery
Texas A&M University
Dept. of Civil Engineering
College Station, Texas 77840

Prof. W.D. Pilkey
University of Virginia
Dept. of Aerospace Engineering
Charlottesville, Virginia 22903

Dr. H.G. Schaeffer
University of Maryland
Aerospace Engineering Dept.
College Park, Maryland 20742

Prof. K.D. Willmert
Clarkson College of Technology
Dept. of Mechanical Engineering
Potsdam, N.Y. 13676

Dr. J.A. Stricklin
Texas A&M University
Aerospace Engineering Dept.
College Station, Texas 77843 ·

Dr. L.A. Schmit
University of California, LA
School of Engineering & Applied Sci.
Los Angeles, California 90024

Dr. H.A. Kamel
The University of Arizona
Aerospace & Mech. Engineering Dept.
Tucson, Arizona 85721

Dr. B.S. Berger
University of Maryland
Dept. of Mechanical Engineering
College Park, Maryland 20742

Prof. G.R. Irwin
Dept. of Mechanical Engng.
University of Maryland
College Park, Maryland 20742

Dr. S.J. Fenves
Carnegie-Mellon University
Dept. of Civil Engineering
Schenley Park
Pittsburgh, Pennsylvania 15213

Dr. Ronald L. Huston
Dept. of Engineering Analysis
Mail Box 112
University of Cincinnati
Cincinnati, Ohio 45221

Prof. George Sih
Dept. of Mechanics
Lehigh University
Bethlehem, Pennsylvania 18015

Prof. A.S. Kobayashi
University of Washington
Dept. of Mechanical Engineering
Seattle, Washington 98105

Librarian
Webb Institute of Naval Architecture
Crescent Beach Road, Glen Cove
Long Island, New York 11542

Prof. Daniel Frederick
Virginia Polytechnic Institute
Dept. of Engineering Mechanics
Blacksburg, Virginia 24061

Prof. A.C. Eringen
Dept. of Aerospace & Mech. Sciences
Princeton University
Princeton, New Jersey 08540

Dr. S.L. Koh
School of Aero., Astro. & Eng. Sc.
Purdue University
Lafayette, Indiana 47907

Prof. E.H. Lee
Div. of Engrg. Mechanics
Stanford University
Stanford, California 94305

Prof. R.D. Mindlin
Dept. of Civil Engrg
Columbia University
S.W. Mudd Building
New York, N.Y. 10027

Prof. S.B. Dong
University of California
Dept. of Mechanics
Los Angeles, California 90024

Prof. Burt Paul
University of Pennsylvania
Towne School of Civil & Mech Engr
Rm. 113 - Towne Building
220 S. 33rd Street
Philadelphia, Pennsylvania 19104

Prof. J.W. Liu
Dept. of Chemical Engr. & Metal.
Syracuse University
Syracuse, N.Y. 13210

Prof. S. Bodner
Technion R&D Foundation
Haifa, Israel

Prof. R.J.H. Bollard
Chairman, Aeronautical Engr. Dept.
207 Guggenheim Hall
University of Washington
Seattle, Washington 98105

Prof. G.S. Heller
Division of Engineering
Brown University
Providence, Rhode Island 02912

Prof. Werner Goldsmith
Dept. of Mechanical Engineering
Div. of Applied Mechanics
University of California
Berkeley, California 94720

Prof. J.R. Rice
Division of Engineering
Brown University
Providence, R.I. 02912

Prof. R.S. Rivlin
Center for the Application of
    Mathematics
Lehigh University
Bethlehem, Pennsylvania 18015

Bell Telephone Labs Inc.
505 King Avenue -Tech. Lib.
Columbus, OH 43201

Dr. Francis Cozzarelli
Div. of Interdisciplinary
    Studies & Research
School of Engineering
State University of New York
Buffalo, N.Y. 14214

Industry and Research Institutes

Library Services Dept.
Report Section Bldg. 14-14
Argonne National Laboratory
9700 S. Cass Avenue
Argonne, Illinois 60440

Dr. M.C. Junger
Cambridge Acoustical Associates
129 Mount Auburn St.
Cambridge, Massachusetts 02138

Dr. L.H. Chen
General Dynamics Corporation
Electric Boat Division
Groton, Connecticut 06340

Dr. J.E. Greenspon
J.G. Engineering Research Assoc.
3831 Menlo Drive
Baltimore, Maryland 21215

Dr. S. Batdorf
The Aerospace Corp.
P.O. Box 92957
Los Angeles, California 90009

Dr. K.C. Park
Lockheed Palo Alto Research Lab.
Dept. 5233, 31dg. 205
3251 Hanover St.
Palo Alto, CA 94304

Library
Newport News Shipbuilding & Dry
    Dock Company
Newport News, Virginia 23607

Dr. W.F. Bozich
McDonnell Douglas Corporation
5301 Bolsa Avenue
Huntington Beach, CA 92647

Dr. H.N. Abramson
Southwest Research Institute
Technical Vice President
Mechanical Sciences
P.O. Drawer 28510
San Antonio, Texas 78284

Dr. R.C. DeHart
Southwest Research Institute
Dept. of Structural Research
P.O. Drawer 28510
San Antonio, Texas 78284

Dr. M.L. Baron
Weidlinger Associates, Consulting
    Engineers
110 East 59th Street
New York, N.Y. 10022

Dr. W.A. Von Riesmann
Sandia Laboratories
Sandia Base
Albuquerque, New Mexico 97115

Dr. T.L. Geers
Lockheed Missiles & Space Co.
Palo Alto Research Laboratory
3251 Hanover Street
Palo Alto, California 94304

Dr. J.L. Tocher
Boeing Computer Services, Inc.
P.O. Box 24346
Seattle, Washington 98124

Mr. William Caywood
Code BBE, Applied Physics Laboratory
8621 Georgia Avenue
Silver Spring, Maryland 20034

Mr. P.C. Durup
Lockheed-California Company
Aeromechanics Dept., 74-43
Burbank, California 91503

Assistant Chief for Technology
Office of Naval Research, Code 200
Arlington, Virginia 22217

Los Alamos Scientific Lab
P.O. Box 1663 - Tech Labs
Los Alamos, NM 87544

Boeing Company
Attn. Aerospace Lab
P.O. Box 3707
Seattle, WA 98124

IIT Research Institute
10 West 35th Street
Chicago, ILL 60616

REPORT DOCUMENTATION PAGE		READ INSTRUCTIONS BEFORE COMPLETING FORM
1. REPORT NUMBER 45	2. GOVT ACCESSION NO.	3. RECIPIENT'S CATALOG NUMBER
4. TITLE (and Subtitle) DIRECT DETERMINATION OF FLEXURAL STRAINS IN PLATES USING PROJECTED GRATINGS		5. TYPE OF REPORT & PERIOD COVERED
		6. PERFORMING ORG. REPORT NUMBER
7. AUTHOR(s) C. Y. Liang, Y. Y. Hung, A. J. Durelli and J. D. Hovanesian		8. CONTRACT OR GRANT NUMBER(s)
9. PERFORMING ORGANIZATION NAME AND ADDRESS Oakland University Rochester, MI 48063		10. PROGRAM ELEMENT, PROJECT, TASK AREA & WORK UNIT NUMBERS
11. CONTROLLING OFFICE NAME AND ADDRESS Office of Naval Research Department of the Navy Washington, D.C. 20025		12. REPORT DATE June 1977
		13. NUMBER OF PAGES 30
14. MONITORING AGENCY NAME & ADDRESS(if different from Controlling Office)		15. SECURITY CLASS. (of this report)
		15a. DECLASSIFICATION/DOWNGRADING SCHEDULE

16. DISTRIBUTION STATEMENT (of this Report)

Distribution of this report is unlimited

17. DISTRIBUTION STATEMENT (of the abstract entered in Block 20, if different from Report)

18. SUPPLEMENTARY NOTES

19. KEY WORDS (Continue on reverse side if necessary and identify by block number)

Moiré   Double differentiation
Projected grating
Flexural strain
Principal strains

20. ABSTRACT (Continue on reverse side if necessary and identify by block number)

It is proposed in this paper to use projected gratings to determine principal strains in plates subjected to bending. The method requires the rotation of one photograph of the deformed grating over a copy of itself, the rotation taking place about the point at which the bending strains are desired. The idea previously suggested by Stetson to double differentiate holograms of bent plates has been extended and verified with an application to a plate subjected to twisting. The proposed method is easy to use and

DD FORM 1473 EDITION OF 1 NOV 65 IS OBSOLETE
1 JAN 73
S/N 0102-014-6601

permits the determination of pricnipal strains in plates subjected to much larger deflections than the ones that can be studied using holograms. Suggestions to improve the precision of the determination are also made.